Multilayer adsorption and desorption: Cs and Li on Ru(0001)

S. H. Payne, H. A. McKay, and H. J. Kreuzer
Department of Physics, Dalhousie University, Halifax, Nova Scotia, Canada B3H 3J5

M. Gierer, H. Bludau, H. Over, and G. Ertl
Fritz-Haber-Institut der Max-Planck-Gesellschaft, Faradayweg 4-6, D-14195 Berlin, Germany
(Received 22 January 1996; revised manuscript received 27 March 1996)

We use a multilayer lattice gas model for adsorption and desorption to analyze and simulate desorption data for Li and Cs on Ru(0001) extracting surface binding energies and lateral interactions. The latter are repulsive for the first layer and attractive for subsequent ones. [S0163-1829(96)03031-7]

I. INTRODUCTION

Whereas adsorbates with mainly repulsive lateral interactions, such as CO on noble or transition metals, are generally restricted to the submonolayer regime, alkali metals adsorbed on most metals exhibit more complex behavior in that their repulsion in the first layer changes to attraction in subsequent layers, which is a necessary feature for bulk growth. A recent study of Li on Ru(0001) (Ref. 1) has revealed an interesting feature in the desorption kinetics, namely, that the second-layer peak in the thermal-desorption spectra continues to grow as the initial coverage is raised beyond second-layer *saturation*. Such a behavior had been predicted in a theoretical approach to multilayer kinetics based on a lattice-gas model.[2] We have previously used this theory to analyze metal-on-metal systems with predominantly attractive interactions which exhibit phase coexistence below or in the desorption range.[3] In this paper we will use this theory to fit and analyze the experimental data for Cs on Ru(0001),[4,5] and also for Li on Ru(0001).[1]

Our main interest is in the adsorption and desorption kinetics of the first few layers, where effects of the adsorbate-substrate interaction are still at play. Alkali-metal systems have strong lateral repulsions in the submonolayer regime which lead to the formation of evenly dispersed adlayers that exhibit a variety of ordered structures at low temperatures. For example, on Ru(0001) alkali adsorbates order in a 2×2 phase at $\theta_S=0.25$, and in a $(\sqrt{3}\times\sqrt{3})R30°$ at $\theta_S=0.33$.[6] Here the coverage θ_S is defined as the ratio of the density of adatoms to that of Ru substrate atoms. Growth of the next 2–3 layers is layer by layer (Frank–van der Merwe).

In Sec. II we first give arguments for our choice of a lattice-gas model, and then briefly outline the theory of adsorption-desorption kinetics for gas-solid systems maintained in quasiequlibrium by fast surface diffusion. In Sec. III we present the results of our analysis of the Cs-Ru(0001) system, followed in Sec. IV with the results for Li on Ru(0001).

II. THEORY

To model such systems with a lattice gas, one starts from the clean Ru surface, defining unit cells with one or more adsorption sites. It is known[6] that in the $(\sqrt{3}\times\sqrt{3})R30°$ structure all alkalis adsorb on Ru(0001) at threefold hcp sites, but for the 2×2 structure adsorption is at the threefold fcc sites for K, Na, and Rb, whereas Cs adsorbs at on-top sites. Thus a model with two binding sites per unit cell would be appropriate. However, there does not seem to be a coverage regime with an ordered phase involving both adsorption sites. Moreover, the formation of incommensurate structures, e.g., for Li and Na, suggests that the lateral corrugation is weak, and that the difference in the binding energies for different adsorption sites is small. We therefore restrict ourselves to a one-site model, also for computational expediency.

For Li only the $(\sqrt{3}\times\sqrt{3})R30°$ structure at $\theta_S=\frac{1}{3}$ is firmly established. For higher coverages compressional effects show up clearly for coverages beyond $\theta_S=0.61$ up to monolayer saturation at 0.78. At any given coverage such a compressional phase can be modeled by an enlarged unit cell with several adsorption sites. In a LEED analysis the structure at $\theta_S=0.64$ was modeled using a 5×1 or a 5×5 unit cell with four and 16 inequivalent adsorption sites, respectively.[1] This suggests a four- or 16-site lattice-gas model which, however, would become inappropriate when the coverage is increased and an even larger unit cell is needed. In addition, there is evidence of mass transfer from the first layer to the second if more than one layer is adsorbed. This means that the density in the first layer is also a function of the presence of subsequent layers. This again requires a model more complex than we need to describe the essential features. We will therefore employ a one-site model for Li on Ru(0001) as well, and choose nearest- and next-nearest-neighbor repulsions so strong that the first layer saturates at a coverage $\theta_S=\frac{3}{4}$, ignoring the details of the compressional phase altogether. Our theory is then based on a lattice-gas model with a Hamiltonian[2]

$$H=[E_{s1}+V_{\rm dip}(\theta)]\sum_i n_i+E_{s2}\sum_i n_i m_i+\tfrac{1}{2}V_{11}\sum_{\rm n.n.} n_i n_j$$
$$+\tfrac{1}{2}V'_{11}\sum_{\rm n.n.n.} n_i n_j+V_{12}\sum_{\rm n.n.} n_i m_i n_j+\tfrac{1}{2}V_{22}\sum_{\rm n.n.} n_i m_i n_j m_j$$
$$+\tfrac{1}{2}V'_{22}\sum_{\rm n.n.n.} n_i m_i n_j m_j+\cdots . \quad (1)$$

Here the occupation number $n_i=0$ or 1 depending on whether site i is empty or has a particle adsorbed in the first

layer with a single-particle energy E_{s1}. Likewise, $m_i=0$ or 1 depending on whether site i in the second layer is empty or occupied with an energy E_{s2}, and so on for additional layers. We assume on-top sites for the second layer, as this is by far the simpler calculation, and we do not expect drastic changes as one goes to multicoordinated higher-layer sites. In (1) we identify V_{11} (V'_{11}) and V_{22} (V'_{22}) as the lateral interactions between two particles in nearest-neighbor (next-nearest-neighbor) sites in the first and second layers, respectively. The interaction V_{12} is between next-nearest neighbors with one particle in the first layer, and the second in the second layer. The nearest-neighbor interaction between a particle in the first layer and another one on top of it in the second layer is accounted for by E_{s2}, which also contains the residual interaction with the substrate. Similar terms have to be added to (1) to account for additional layers. Since the lattice-gas Hamiltonian should give the same Helmholtz free energy as a microscopic Hamiltonian (for noninteracting particles), one can show that[7]

$$E_{s1}=-V_0^{(1)}-k_BT\ \ln(q_3^{(1)}), \tag{2}$$

with a similar expression for E_{s2}. Here $V_0^{(1)}$ is the (positive) binding energy of an isolated adparticle in the first layer. $V_0^{(2)}$ is the binding energy of a single adparticle in the second layer atop an isolated particle in the first layer, i.e., the difference $V_0^{(2)}-V_0^{(1)}$ accounts for the interaction between these particles and the shielding action of the first layer on the interaction of the second layer with the substrate. q_3 is a partition function for the vibrations of the adparticle with respect to the substrate, which we approximate by three harmonic oscillators of frequencies ν_z and $\nu_x=\nu_y$, respectively, accounting for the motion perpendicular and parallel to the surface. The mean-field term $V_{\rm dip}(\theta)\Sigma_i n_i$ is introduced to account for the long-ranged dipole-dipole interactions; it will be discussed below.

To model the adsorption-desorption kinetics we can safely assume that fast surface diffusion (fast on the time scale of adsorption and desorption) maintains the adsorbate in quasiequilibrium. In such situations the system is completely characterized by the coverage $\theta=\theta_S$, and we get the adsorption and desorption rates to be[2,8,9]

$$R_{\rm ad}=S(\theta,T)a_s\,\frac{\lambda}{h}\,P, \tag{3}$$

$$R_{\rm des}=S(\theta,T)a_s\,\frac{k_BT}{h\lambda^2 q_3}\,e^{[-V_0^{(1)}+\mu_{\rm ad}(\theta,T)]/k_BT}, \tag{4}$$

with a_s the area of an adsorption site, $\lambda=h/(2\pi m k_BT)^{1/2}$ the thermal wavelength of the adparticle of mass m, $S(\theta,T)$ the sticking coefficient, and P the instantaneous pressure. The dependence of the desorption rate on the binding difference $\Delta V_{n,n+1}=V_0^{(n)}-V_0^{(n+1)}$, and the lateral interaction energies such as V_{11}, V_{22}, etc., is accounted for in the chemical potential $\mu_{\rm ad}(\theta,T)$. The binding difference $\Delta V_{n,n+1}$ approaches zero beyond the first few layers.

To complete the theory we need (i) to specify the coverage dependence of the sticking coefficient, and (ii) to calculate the chemical potential of the adsorbate from the Hamiltonian (1). The sticking coefficient is a measure of the efficiency of energy transfer in adsorption and desorption. Thus it must be calculated from a microscopic theory or be postulated in a phenomenological approach, based on experimental evidence for a particular system or some simple arguments. For interacting systems it is generally both coverage and temperature dependent. For metals on metals the sticking coefficient is observed to be independent of coverage, and we will assume this below.

We obtain the chemical potential by employing the transfer-matrix method.[2] The transfer matrix is constructed for interactions between particles in two adjacent rows of M adsorption sites in the finite direction. Its leading eigenvalue λ_1 gives the grand partition function, and the coverage θ is obtained from the corresponding eigenvector. The partial coverages of the first two layers are given by $\theta_1=\Sigma_i\langle n_i\rangle$ and $\theta_2=\Sigma_i\langle m_i\rangle$. Exact results can be obtained by this method for large enough M. We have performed all our calculations for $M=6$ on a hexagonal lattice.

III. Cs ON Ru(0001)

We now turn to our first system, Cs on Ru(0001).[4,5] Experimental TPD (temperature-programmed desorption) traces[4,5] for up to three monolayers of adsorbate are reproduced in Figs. 1(a)–1(c). There is some discrepancy in these data in that Hrbek's data has desorption complete below 1100 K, whereas the newer data in Fig. 1(a) have desorption proceeding even beyond 1200 K. In these figures the first, second, and third layers are completed at coverages 0.33, 0.56, and 0.85. Because we ignore the expansion in the second layer, i.e., the increase in the Cs lattice constant, the completion of these three layers in our lattice-gas model occurs at rescaled coverages $\frac{1}{3}$, $\frac{2}{3}$, and 1. In Figs. 1(d)–1(f) we show a theoretical fit to these TPD data, for the equivalent initial coverages, obtained as follows: the low-coverage ($\theta\simeq 0.01$) desorption trace is mainly determined by the binding energy of an isolated atom to the surface, $V_0^{(1)}$, and its vibrational frequencies parallel ($\nu_x=\nu_y$) and perpendicular (ν_z) to the substrate. The perpendicular Cs-Ru vibration has been determined by high-resolution electron-energy-loss spectroscopy[10] to be $\nu_z=1.8\times10^{12}\ \mathrm{s}^{-1}$, and the parallel vibration has been estimated from a low-energy electron-diffraction analysis of the Ru(0001)$-(2\times2)$-Cs structure[6,11] to be in the range 3–$5\times10^{11}\ \mathrm{s}^{-1}$. We thus have one free parameter to fit the peak position in TPD at the lowest coverage, and obtain $V_0^{(1)}=3.1$ eV for the binding energy of a single Cs atom to the Ru surface.

We next note that desorption from an initial coverage of $\frac{1}{4}$ peaks around 600 K. In order to reproduce this feature by a next-nearest-neighbor interaction only, its strength would have to be of the order of the binding energy itself. Even then the low initial coverage curves would be in disagreement with the experimental data, which show rather broad desorption traces. On inhomogeneous surfaces such long tails in the TPD traces are sometimes attributable to adsorption in a continuum of energetically close adsorption sites. However, for alkali-metal adsorption we know that at low coverage an evenly dispersed adlayer is formed due to the long-range Coulomb or dipole repulsion between (charged) adatoms. This should be included in the lattice-gas model by additional interactions between third, fourth, etc. neighbors. However, this introduces too many parameters, and also be-

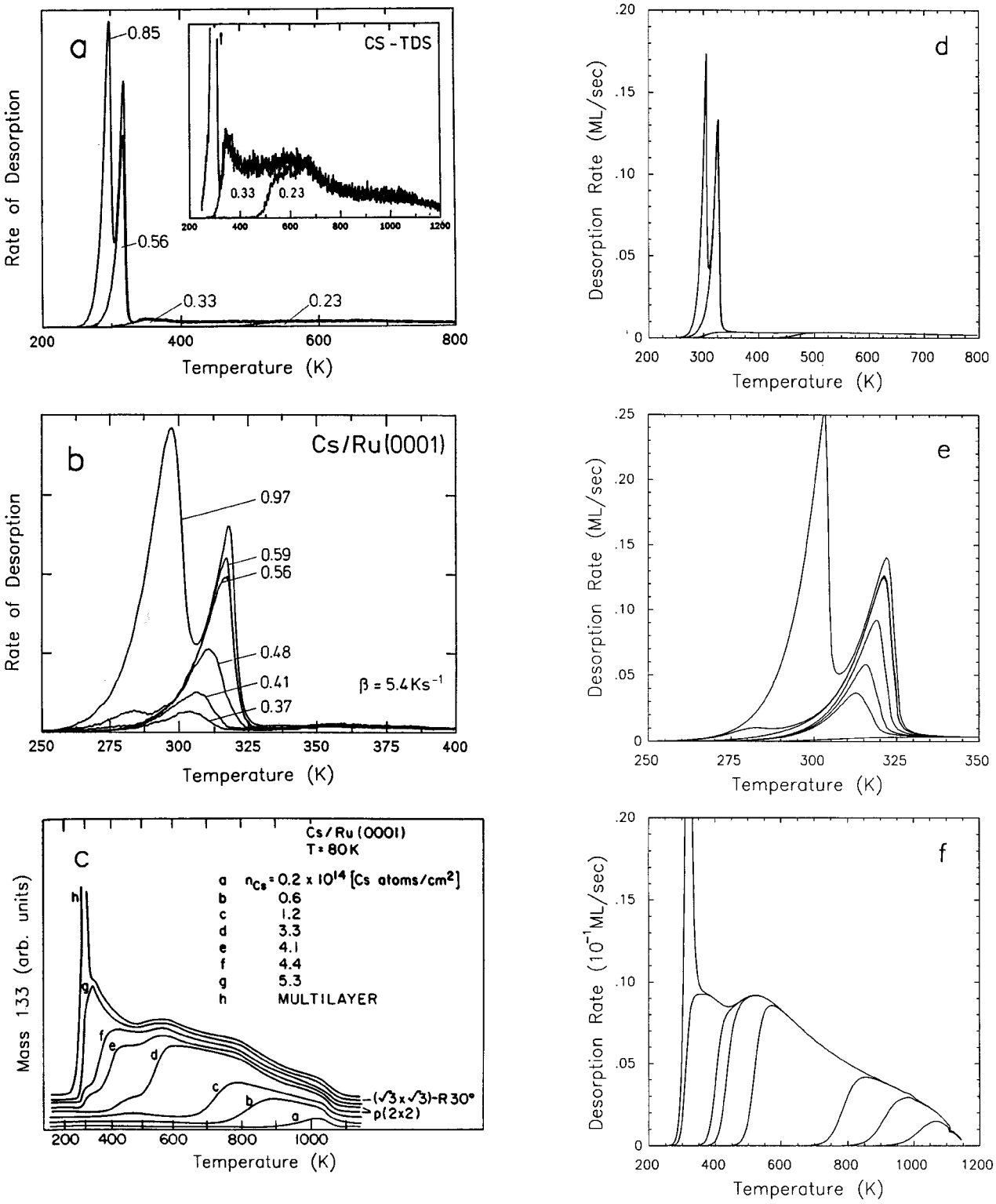

FIG. 1. (a) TPD data for the first three layers of Cs on Ru(0001) obtained with a heating rate of 5.4 K s^{-1} (Ref. 4). (b) TPD for second and third layers with 5.4 K s^{-1} (Ref. 4). (c) TPD for first layer with 15 K s^{-1} (Ref. 5). The theoretical fit to these data are with the following parameters: $V_0^{(1)}=3.1$ eV, $V_0^{(2)}=2.67$ eV, $V_0^{(3)}=2.59$ eV, $V_{11}=V_{12}=0.172$ eV, $V'_{11}=0.02$ eV, $V_{22}=V_{33}=0.05$ eV, $V'_{22}=-0.05$ eV, $V'_{33}=-0.06$ eV, $\nu_z=1.8\times10^{12}$ s^{-1}, and $\nu_x=\nu_y=3\times10^{11}$ s^{-1}. Initial coverages in the lattice gas $\theta_0=1.0$, 0.66, 0.33, and 0.23 for (d), 1.14, 0.69, 0.66, 0.56, 0.48, and 0.43 for (e), and 0.4, 0.33, 0.27, 0.25, 0.20, 0.074, 0.037, and 0.012 for (f). Experimental data reproduced with permission from The Physical Review and Surface Science.

comes computationally impractical. We have therefore included the long-range interactions summarily by adding a mean-field term to the Hamiltonian, $V_{\rm dip}(\theta)\,\Sigma n_i$. To account for the fact that the dipole moment of the adsorbed alkali atoms decreases as a function of coverage, as evidenced by the coverage dependence of the work function,[6] we have made the strength $V_{\rm dip}$ coverage dependent, as shown in Fig. 2(a), to accomplish a good fit to the TPD traces for low

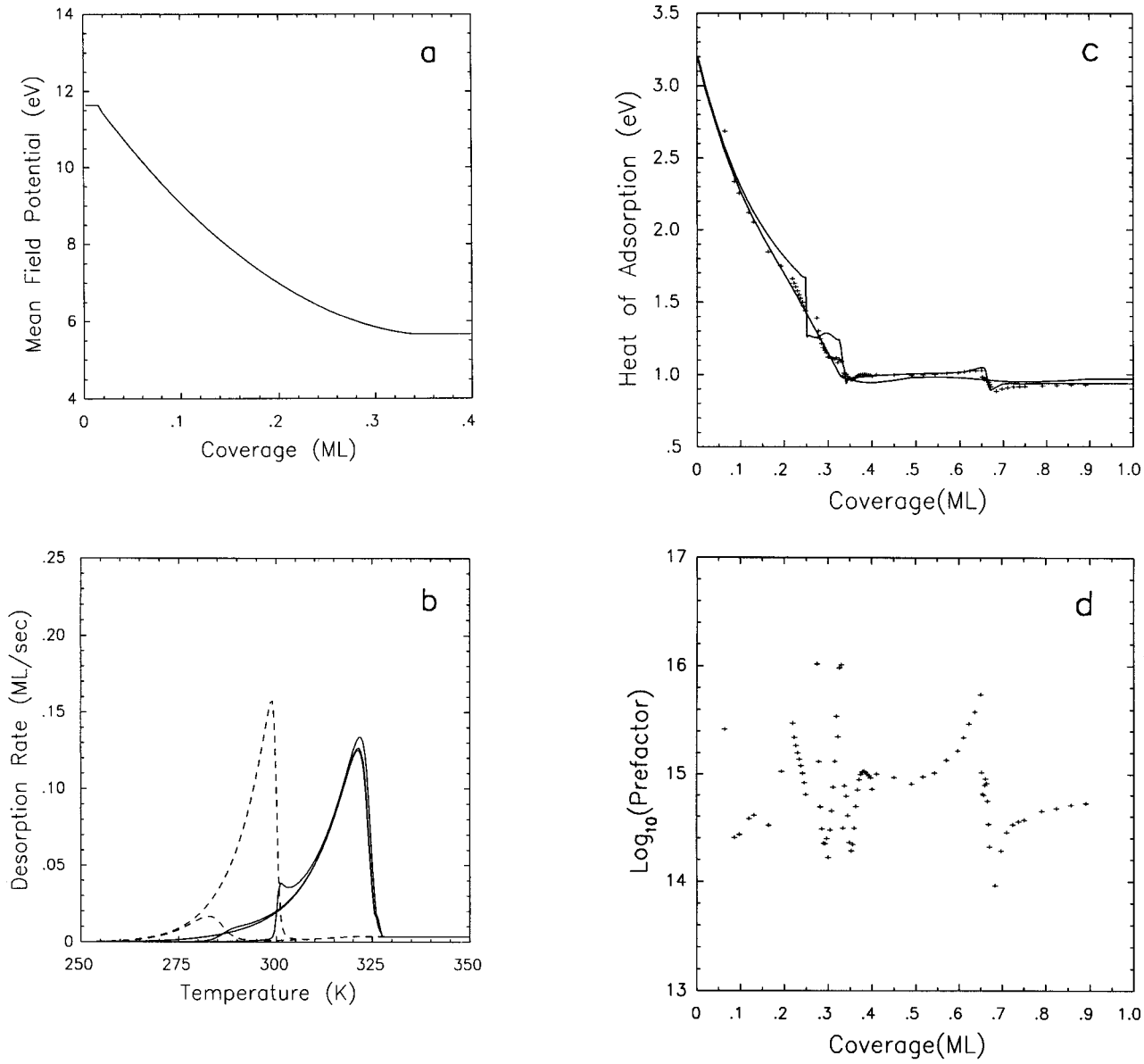

FIG. 2. (a) Variation of mean-field energy $V_{\mathrm{dip}}(\theta)$, with coverage for Cs on Ru(0001). (b) Partial rates $d\theta_2/dt$ (solid) and $d\theta_3/dt$ (dashed) for initial coverages of 0.95, 0.69, and 0.66 corresponding to Fig. 1. (c) Isosteric heat of adsorption for $T=250$ and 700 K (top to bottom at $\theta=0.2$). Crosses mark the desorption energy obtained from an isosteric Arrhenius analysis of the theoretical TPD curves (Fig. 1), and (d) the corresponding effective prefactor from this analysis.

initial coverages. One may interpret this coverage dependence as arising from dipole-dipole repulsion of the atoms in concert with a modification of the single-atom binding energy due to the change in the image potential (as long as one keeps in mind that only the coverage dependence of the total energy of the system is an observable quantity, and that any separation into single- and two-particle terms is arbitrary).

To account for the 2×2 structure at coverage $\theta=\frac{1}{4}$, and the corresponding hump in TPD around 500 K, we determine a weak next-nearest-neighbor repulsion $V'_{11}=0.02$ eV. A nearest-neighbor repulsion $V_{11}=0.172$ eV next ensures that an ordered $(\sqrt{3}\times\sqrt{3})$ structure forms at $\theta=\frac{1}{3}$ at low temperature, and, similarly, ensures a correct positioning of the TPD traces around this coverage.

Because the TPD traces for the second and third layers are narrow on the scale of the first-layer desorption, it is relatively easy to determine the binding-energy differences for isolated atoms in these layers. Taking account of the interactions necessary to fit the desorption features of Fig. 1(b), we obtain $\Delta V_{12}=V_0^{(1)}-V_0^{(2)}=0.564$ eV and $\Delta V_{23}=0.082$ eV. We have chosen the vibrational frequencies for adatoms in the higher layers to equal those in the first layer, for simplicity. One expects them to eventually approach bulk values. Saturation of the first layer occurs at coverage $\frac{1}{3}$ because for $\Delta V_{12}<3V_{11}$ a second layer forms beyond this coverage rather than adparticles settling into nearest-neighbor sites in the first layer. Nearest-neighbor interactions in the second and third layers must be repulsive to maintain the correct Cs density relative to the Ru substrate. Next-nearest-neighbor interactions (which are nearest-neighbor interactions within the Cs lattice) are necessarily attractive to stabilize these layers (i.e., make them metallic) and to reproduce the rather narrow desorption peaks for the second and third layers

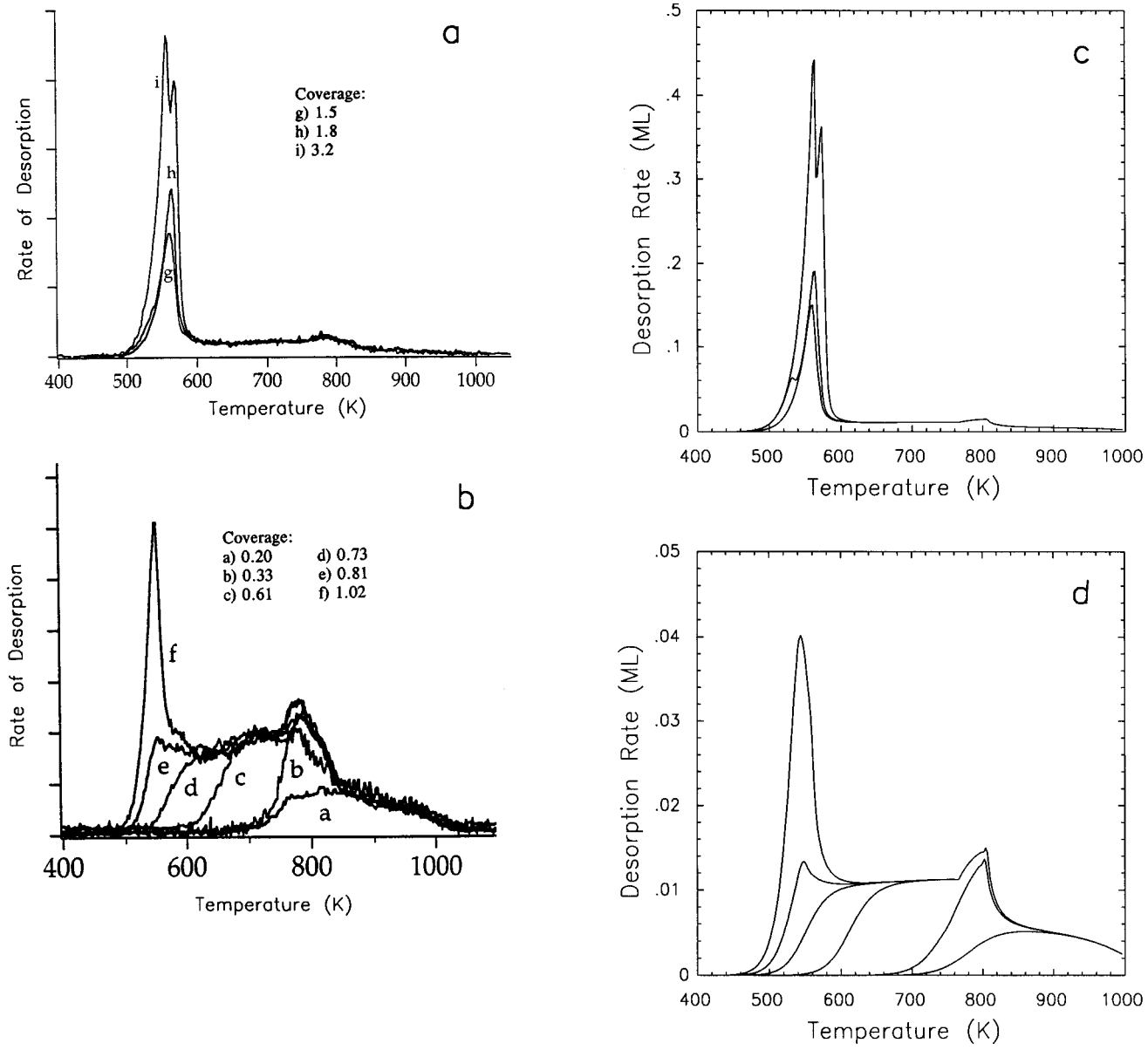

FIG. 3. (a) and (b) TPD data for the first four layers of Li on Ru(0001) obtained with a heating rate of 5.4 K s^{-1} (Ref. 1). (c) and (d) Theoretical fit with the following parameters: $V_0^{(1)}=2.86$ eV, $V_0^{(2)}=2.13$ eV, $V_0^{(3)}=V_0^{(4)}=2.1$ eV, $V_{11}=0.086$ eV, $V'_{11}=0.006$ eV, $V_{22}=V_{33}=V_{44}=-0.05$ eV, and $\nu_x=\nu_y=\nu_z=5.2\times10^{12}$ s^{-1}.

around $T=320$ and 300 K, respectively.

Although one can never claim the uniqueness of a model as long as a limited set of data is available for a fit, we can say that within the current lattice-gas model the interaction parameters are fixed within an uncertainty of less than 20% as any larger variation will lead to qualitative changes in the TPD spectra. For example, the particular dependence of the mean field $V_{\rm dip}$ on coverage cannot be varied much from the form given in Fig. 2(a): to reproduce the lowest three TPD traces it is necessary that $V_{\rm dip}$ remains constant up to coverage 0.02, in agreement with the fact that the experimental dipole moment remains constant in this range. Its value here is also consistent with the dipole energy.[6] The subsequent decrease then mimics the higher coverage dependence of the dipole moment.

The growth mode of the Cs film is layer by layer, despite the overlap of the second- and third-layer TPD peaks. This has an interesting consequence for the partial rates $d\theta_i/dt$, Fig. 2(b), in the intermediate-temperature range of TPD: the partial rates show almost independent desorption of the two layers, with the second layer trailing the third at higher temperatures. A close inspection of the TPD spectra in Figs. 1(b) and 1(e) reveals that the desorption peak of the second layer does not saturate for coverages up to two Cs monolayers. The explanation that comes to mind is simultaneous desorption from the second and third layers. However, this would not produce two separate peaks. The proper explanation is as follows:[2] because the binding-energy difference between the second and third layers is rather small, the third-layer desorption peak occurs on the leading edge of the second layer. Desorption from the second layer is thus constrained by that of the third, resulting in an additional small shift of the second layer peak for initial coverages larger than two Cs monolayers to higher temperatures, as compared to desorp-

tion from just 2 ML. We illustrate this explicitly in Fig. 2(b) for initial coverages $\theta_0=0.66$ and 0.95, i.e., 2.0 and 2.9 Cs ML. The presence of the third layer suppresses the desorption of a fraction of the second layer, which desorbs instead at higher temperatures. Thus the second-layer peak continues to grow in height beyond coverages slightly larger than 2 ML. For adsorption of several layers the chemical potential will tend toward its bulk value, which implies that the low-temperature peak extends to higher rates and somewhat higher temperatures.

In Fig. 2(c) we show the isosteric heat of adsorption

$$Q_{\rm iso}(\theta,T)=k_BT^2\left.\frac{\partial \ln P}{\partial T}\right|_{\theta} \tag{5}$$

for the interactions used to fit TPD and for various temperatures. Here P is the equilibrium pressure which maintains a coverage θ at temperature T. The isosteric heat is essentially that of independent layers. Starting at zero coverage and low temperature the sharp drops in $Q_{\rm iso}$ at $\theta_S=\frac{1}{4}$ and $\frac{1}{3}$ reflect the fact that after the 2×2 and $(\sqrt{3}\times\sqrt{3})R30°$ orderings are established, an additional particle will see two next-nearest and nearest neighbors, and three nearest neighbors, respectively. Thus these drops are of magnitude $2(V_{11}+V'_{11})$ and (less than) $3V_{11}$, respectively. However, for our multilayer system the drop is less for the latter because the energetics is such as to favor the formation of the second layer. For $\theta_S>\frac{1}{3}$ the heat of adsorption is essentially constant, reflecting the attractive next-nearest-neighbor interactions in subsequent layers. The slight drop at coverage $\frac{2}{3}$ and at low temperature corresponds to the reduced binding of isolated atoms in the third layer, with the heat of adsorption approaching its bulk value, i.e., the heat of sublimation. Our value of the heat of adsorption, about 0.9 eV, is somewhat larger than the heat of sublimation, about 0.7 eV.

Looking back at the energy parameters in the lattice-gas Hamiltonian, we need to comment on the values for $V_0^{(3)}$ and V'_{33}. At the surface of an ideally terminated bulk crystal one expects the binding energy to the surface ($V_0^{(3)}$ in this case) to be three times the nearest-neighbor bond energy on the (001) surface of a hcp lattice, and the nearest-neighbor lateral interaction (V'_{33} in this case) to be equal to (the negative of) that bond energy. Allowing for surface relaxation on a real crystal, one expects the surface binding to increase slightly, and the lateral interaction to decrease accordingly. These simple rules are obviously not satisfied in our fit for a number of reasons. First, by construction of the lattice-gas Hamiltonian, the binding energy $V_0^{(3)}$ is that of an isolated adatom on top of a stack of identical atoms in the first and second layers. To obtain the binding energy of a single adatom in the third layer on the completed first and second layers, we have to add to $V_0^{(3)}$ the sum total of the lateral interactions in those layers, i.e., the effective binding energy (at $T=0$) is $V_0^{(3)}-0.33V_{\rm dip}(\theta=\frac{1}{3})-3V'_{11}-3V'_{22}\simeq0.75$ eV, i.e., roughly the heat of sublimation or, more properly, the heat of adsorption, as we are not yet dealing with a bulk property at the completion of the third layer. There is no significant contribution to the heat of adsorption from the lateral interactions, because the latter are so much less than the bond energy in bulk. The reason is simply that we are describing alkali layers grown on the (001) surface of a hcp crystal and not a bcc lattice, and that correspondingly the nearest-neighbor distance between Cs atoms in the completed third layer with a $(\sqrt{3}\times\sqrt{3})R30°$ structure, 4.69 Å, is considerably smaller than the value in bulk, 5.24 Å, so that a considerable reduction in bond energy due to the increased repulsion at shorter distances is expected. We want to stress once more that only the total energy of the system or some thermodynamically related quantity, such as the heat of adsorption or sublimation, are physically observable quantities. Any separation of the total energy into single-particle and multiparticle contributions, e.g., surface binding energies and lateral interactions, is based either on intuition or on convenience. The lattice-gas model provides one possible scenario to do this rather systematically.

It is usual to perform an Arrhenius analysis on TPD data extracting the coverage dependence of the desorption energy and of the effective prefactor in the Arrhenius parametrization of the desorption rate, $R_{\rm des}=\nu_{\rm eff}(\theta)\exp[-E_d(\theta)/k_BT]\theta$. We stress that this is a parametrization of data, allowing the separation into an energy (Boltzmann) and an entropy factor. For a system which is kept in quasiequilibrium during desorption by fast surface diffusion, the desorption energy is a temperature average of the isosteric heat of adsorption (displaced by $k_BT/2$), and the prefactor is in part the temperature average of $\exp(\Delta S/k_B)$.[8,9] We have performed an analysis of the theoretical TPD spectra, Figs. 1(d)–1(f), plotting isosteric rates versus T^{-1} and extracting slopes (E_d) and intercepts ($\nu_{\rm eff}$) as a function of coverage.[12] The results are shown in Figs. 2(c) and 2(d). Note that the effective prefactor in this parametrization is strongly coverage dependent, reflecting the variation of the entropy as various layers in the Cs film are completed. The theory from which the desorption rate is calculated is based on the Hamiltonian (1), which as parameters contains constant binding and interaction energies and vibrational frequencies of an adatom with respect to the substrate. Because we calculate the chemical potential, which appears in the desorption rate (4), we have thus calculated the changes in energy (E_d) and entropy ($\ln(\nu_{\rm eff})$) of the system.

IV. Li ON Ru(0001)

We now turn to our second system, Li on Ru(0001),[1] and show experimental TPD data in Figs. 3(a) and 3(b). The major difference from the Cs/Ru(0001) system is the fact that the partial coverage in the first layer now goes up to 0.78 ML, obviously due to a smaller nearest-neighbor repulsion (or a weaker relative binding of particles in the second and higher layers). Strong long-ranged repulsion of a Coulombic or dipolar nature again leads to a high-temperature tail in desorption which we account for via a mean-field term. As discussed above, Li/Ru(0001) is also more complicated compared to Cs/Ru(0001), in that it exhibits a compressional phase in the first layer around coverage $\frac{2}{3}$. In Figs. 3(c) and 3(d) we show a theoretical fit to the data which was obtained similarly to that in Figs. 1(d)–1(f), with the dipole potential given in Fig. 4(a). In particular to get the peak in TPD around 800 K the mean-field energy $V_{\rm dip}(\theta)$ must be constant ($=0.34$ eV) for $0.2<\theta<0.3$. Our lattice-gas model cannot account for the compression of the first layer between coverages $\theta_S\simeq0.61-0.78$, and has the maximum theoretical

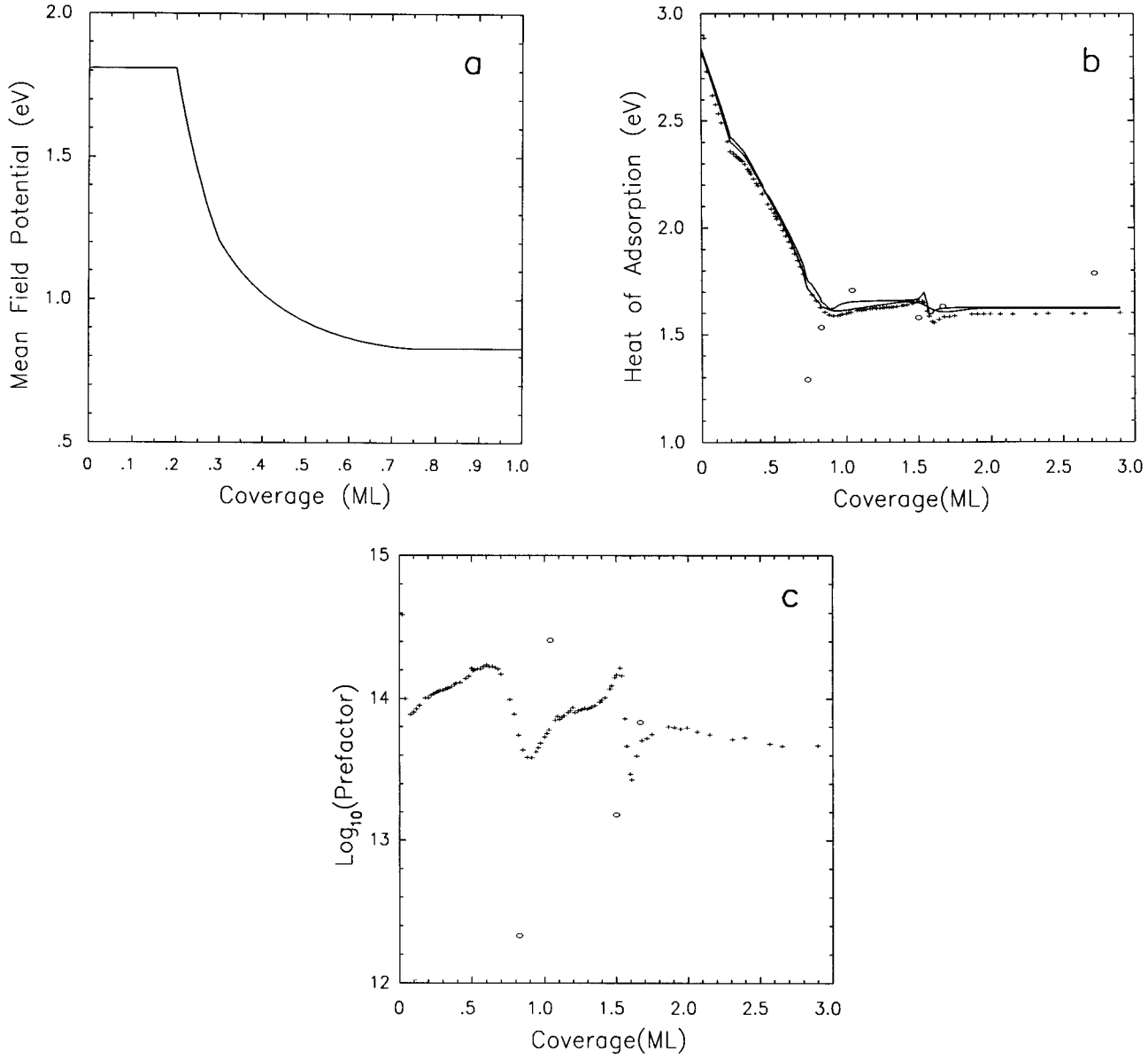

FIG. 4. (a) Variation of mean-field energy $V_{\mathrm{dip}}(\theta)$, with coverage for Li on Ru(0001). (b) Isosteric heat of adsorption for $T=450$ and 700 K (top to bottom at $\theta=1.0$). Crosses mark the desorption energy obtained from an isosteric Arrhenius analysis of the theoretical TPD curves, and open circles are from a threshold analysis (Ref. 12) of the data in Figs. 3(a) and 3(b). (c) Corresponding effective prefactor from these analyses.

coverage in the first layer at $\frac{3}{4}$.

A close inspection of the TPD data again reveals that the second-layer desorption peak does not saturate upon completion of the second layer of Li [between curves *g* and *h* in Fig. 3(a)]. Indeed, in this system this peak rises substantially (to curve *i*) when the third layer forms. As discussed above for Cs, this behavior is due to the fact that the desorption of a fraction of the second layer is suppressed as long as the third layer is still present.

We have performed a threshold analysis[12] of the experimental TPD data, Fig. 3(a) and 3(b), extracting coverage-dependent desorption energies and prefactors as depicted in Figs. 4(b) and 4(c) together with the isosteric heat. Note again that the heat of adsorption at the highest coverage is very close to the heat of sublimation of bulk lithium, 1.53 eV. The experimental data in the long tails of the desorption traces above 850 K, corresponding to low coverages, are too noisy for analysis.

V. SUMMARY

In this paper we have analyzed two systems, Cs/Ru(0001) and Li/Ru(0001), for which a multilayer lattice gas gives excellent fits to TPD data, both in shape and in absolute magnitude of the rates. The theory is essentially exact employing transfer-matrix methods apart from our parametrization of the dipolar energy. The quality of the theoretical fits is nevertheless surprising, as the model assumes on-top adsorption for the second and higher layers, whereas on a hcp(0001) surface the second-layer atoms are threefold coordinated to the first layer. Taking proper account of the coordination will change the numerical value of the second- and

higher-layer binding energies, $V_0^{(2)}$, $V_0^{(3)}$, etc., but will not change the qualitative feature of layer-by-layer growth, as a threefold-coordinated atom in the second layer prevents three first-layer atoms from desorbing, whereas an on-top atom only inhibits the desorption of one.

The essential features of our model of alkali adsorption and desorption, namely, mean-field behavior at low coverage due to long-range Coulomb or dipolar interactions, a changeover from repulsion in the first layer to attraction in higher layers, and the consequent layer-by-layer growth, have been observed on other metals as well.[13] It remains an interesting challenge to theory to obtain the basic binding and interaction energies in the lattice gas for adsorbed alkalis from *ab initio* calculations,[14,15] and to then proceed to calculate equilibrium properties and desorption spectra according to the theory used in this paper.

ACKNOWLEDGMENT

One of us (H.J.K.) acknowledges support through a grant by the Office of Naval Research.

[1] M. Gierer, H. Over, H. Bludau, and G. Ertl, Phys. Rev. B **52**, 2927 (1995).
[2] S. H. Payne and H. J. Kreuzer, Surf. Sci. **338**, 261 (1995).
[3] S. H. Payne, H. J. Kreuzer, A. Pavlovska, and E. Bauer, Surf. Sci. **345**, L1 (1996).
[4] H. Over, H. Bludau, M. Stottke-Klein, G. Ertl, W. Moritz, and C. T. Campbell, Phys. Rev. B **45**, 8638 (1992). See also H. Bludau, Ph.D. thesis, Freie Universität Berlin, 1992.
[5] J. Hrbek, Surf. Sci. **164**, 139 (1985).
[6] H. Over, H. Bludau, M. Gierer, and G. Ertl, Surf. Rev. Lett. **2**, 3 (1995).
[7] H. J. Kreuzer and Zhang Jun, Appl. Phys. A **51**, 183 (1990).
[8] S. H. Payne and H. J. Kreuzer, Surf. Sci. **222**, 404 (1989).
[9] H. J. Kreuzer and S. H. Payne, in *Dynamics of Gas-Surface Collisions*, edited by M. N. R. Ashfold and C. T. Rettner (Royal Society of Chemistry, Cambridge, 1991).
[10] K. Jacobi, H. Shi, M. Gruyters, and G. Ertl, Phys. Rev. B **49**, 5733 (1994).
[11] H. Over, M. Gierer, H. Bludau, and G. Ertl, Phys. Rev. B **52**, 16 812.
[12] The analysis and simulations in the submonolayer regime were performed with the ASTEK package written by H. J. Kreuzer and S. H. Payne (available from Helix Science Applications, Box 49, Site 3, R.R. 5, Armdale N.S. B3L 4J5, Canada).
[13] H. Stolz, M. Höfer, and H.-W. Wassmuth, Surf. Sci. **287/288**, 564 (1993).
[14] M. Scheffler, Ch. Droste, A. Flseszar, F. Maca, G. Wachutka, and G. Barzel, Physica B **172**, 143 (1991).
[15] C. Stampfl, G. Neugebauer, and M. Scheffler, Surf. Sci. **307/309**, 8 (1994).